



Published in final edited form as:

*ACS Appl Bio Mater.* 2020 April 20; 3(4): 2360–2369. doi:10.1021/acsabm.0c00100.

## Extracellular Matrix Proteins and Substrate Stiffness Synergistically Regulate Vascular Smooth Muscle Cell Migration and Cortical Cytoskeleton Organization

**Alex P. Rickel, Hanna J. Sanyour**

Department of Biomedical Engineering, University of South Dakota, Sioux Falls, South Dakota 57107, United States; BIOSNTR, Sioux Falls, South Dakota 57107, United States

**Neil A. Leyda,**

Department of Chemical Engineering, South Dakota School of Mines & Technology, Rapid City, South Dakota 57701, United States

**Zhongkui Hong**

Department of Biomedical Engineering, University of South Dakota, Sioux Falls, South Dakota 57107, United States; BIOSNTR, Sioux Falls, South Dakota 57107, United States

### Abstract

Vascular smooth muscle cell (VSMC) migration is a critical step in the progression of cardiovascular disease and aging. Migrating VSMCs encounter a highly heterogeneous environment with the varying extracellular matrix (ECM) composition due to the differential synthesis of collagen and fibronectin (FN) in different regions and greatly changing stiffness, ranging from the soft necrotic core of plaques to hard calcifications within blood vessel walls. In this study, we demonstrate an application of a two-dimensional (2D) model consisting of an elastically tunable polyacrylamide gel of varying stiffness and ECM protein coating to study VSMC migration. This model mimics the *in vivo* microenvironment that VSMCs experience within a blood vessel wall, which may help identify potential therapeutic targets for the treatment of atherosclerosis. We found that substrate stiffness had differential effects on VSMC migration on type 1 collagen (COL1) and FN-coated substrates. VSMCs on COL1-coated substrates showed significantly diminished migration distance on stiffer substrates, while on FN-coated substrates VSMCs had significantly increased migration distance. In addition, cortical stress fiber orientation increased in VSMCs cultured on more rigid COL1-coated substrates, while decreasing on stiffer FN-coated substrates. On both proteins, a more disorganized cytoskeletal architecture was associated with faster migration. Overall, these results demonstrate that different ECM proteins

---

**Corresponding Author: Zhongkui Hong** – Department of Biomedical Engineering, University of South Dakota, Sioux Falls, South Dakota 57107, United States; BIOSNTR, Sioux Falls, South Dakota 57107, United States; Zhongkui.Hong@usd.edu.

Author Contributions

All authors have given approval to the final version of the manuscript.

Supporting Information

The Supporting Information is available free of charge at <https://pubs.acs.org/doi/10.1021/acsabm.0c00100>.

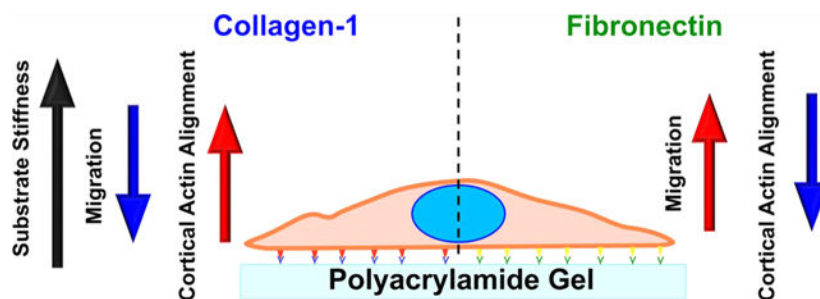
ECM protein-coating evaluation; AFM image analysis: fiber density and orientation; ECM protein-coated gels (Figure S1); AFM height image flattening (Figure S2); calculation of *x*- and *y*-gradients of the AFM deflection image (Figure S3) (PDF)

Complete contact information is available at: <https://pubs.acs.org/doi/10.1021/acsabm.0c00100>

The authors declare no competing financial interest.

can cause substrate stiffness to have differential effects on VSMC migration in the progression of cardiovascular diseases and aging.

## Graphical Abstract



## Keywords

vascular smooth muscle cell; migration; polyacrylamide gel; cytoskeleton; atherosclerosis

## 1. INTRODUCTION

Vascular smooth muscle cells (VSMCs) are the primary cellular constituent of the medial layer of arteries, contributing to vascular tone and blood pressure regulation. It has long been known that VSMCs undergo phenotypic switching from a quiescent contractile phenotype to a synthetic phenotype with aging and cardiovascular diseases such as atherosclerosis.<sup>1-3</sup> With the synthetic phenotype, VSMCs acquire an increased capacity for proliferation, migration, and extracellular matrix (ECM) protein secretion.<sup>1</sup> VSMC migration and proliferation are critical to the formation of the fibrous cap in atherosclerotic plaques and intimal thickening that occurs with age.<sup>1,4</sup> In addition, VSMCs have been found to make up a large portion of the necrotic plaque core. The core of a plaque is occupied by lipid-laden macrophages known as foam cells. However, VSMC-derived foam cells have been found to comprise up to 40% of the total foam cells.<sup>5</sup>

Migrating VSMCs encounter a broad range of microenvironments as the ECM varies widely within atherosclerotic plaques and with aging, both in composition and stiffness. Tracqui et al. used atomic force microscopy (AFM) to measure the stiffness of different regions of plaques in apolipoprotein E-deficient (ApoE) mice, finding stiffness varied from a low average of 5.5 kPa in lipid-rich regions to an average of 59 kPa with high values of 250 kPa in areas of hypocellular fibrosis.<sup>6</sup> Calcifications, another key feature of advanced plaques, especially in older patients, are considerably stiffer, reaching the GPa range.<sup>4,7,8</sup> Elsewhere, stiffer ECMs have been shown to promote angiogenesis.<sup>9,10</sup> It has been well established that stiffening of arteries also occurs with age, due in large part to a change in ECM composition and in particular an increased collagen to elastin ratio.<sup>2,4</sup> It has also been reported that increased transforming growth factor- $\beta$ 1 expression in aged rat aortas resulted in increased expression of fibronectin (FN), type I collagen (COL1), and type III collagen.<sup>11,12</sup> Within an atherosclerotic plaque, a varied ECM composition occurs in different regions. COL1 is highly prevalent within the fibrous cap but nearly absent from the lipid-rich core, and

increased FN deposition has been associated with early atherosclerotic lesions and VSMC remodeling.<sup>13</sup> Furthermore, migrating cells have been shown to actively modify the ECM, promoting FN fibril formation, collagen deposition, and strain stiffening of the ECM.<sup>14–16</sup> Given the widely varied ECM environments potentially experienced by migrating VSMCs, deciphering the interplay of ECM stiffness and composition is critical to further understanding of atherosclerosis progression. Previous studies comparing FN and laminin-coated substrates have shown differential responses to substrate stiffness with FN showing enhanced responses and laminin showing depressed responses.<sup>17–20</sup>

Cells are able to sense forces from their surrounding environment and translate mechanical signals into biochemical responses, a process known as mechanotransduction.<sup>21</sup> Binding to the ECM occurs through focal adhesion complexes (FAs), mainly consisting of integrins, which bind directly to the ECM and various intracellular proteins.<sup>21</sup> FAs connect to and transduce mechanical signals to the actin cytoskeleton through mechanosensitive proteins such as talin and vinculin.<sup>21,22</sup> Known as the molecular clutch, the proteins connecting the ECM-bound integrins to actin filaments harness the retrograde motion of actin to generate tension along the substrate to induce movement. This system is sensitive to ECM stiffness as talin unfolding only occurs on stiff substrates, allowing the recruitment of vinculin and higher force transmission.<sup>22</sup> Ample previous studies have demonstrated the ability of the ECM to alter cell fate and function.<sup>23–26</sup> In addition, the transduction of forces to the actin cytoskeleton can induce cytoskeletal remodeling in response to ECM stiffness changes.<sup>27,28</sup>

The stiffness and composition of the ECM are known to affect VSMC migration during atherosclerosis and aging as well as the actin cytoskeleton. However, the combinatorial effect of ECM stiffness and composition is worth further investigation given the varied microenvironments seen in atherosclerosis, especially how they affect migration dynamics and actin cytoskeleton orientation. In this study, we investigated the influence of ECM stiffness and composition on VSMC migration using elastically tunable polyacrylamide (PA) gels coated with COL1 or FN, as well as a novel analysis of migration dynamics. The combinatorial effect of ECM stiffness and composition on cytoskeleton orientation was also studied by confocal microscopy and AFM.

## 2. METHODS

### 2.1. Vascular Smooth Muscle Cell Isolation.

Animals used in this study were kept in accordance with the NIH guidelines (8th Edition of the Guide for the Care and Use of Laboratory Animals), and the animal use protocol was approved by the Laboratory Animal Use Committee of the University of South Dakota (#13-09-15-18C) and Sanford Institutional Care and Use Committee (#153-03-21C). VSMCs were enzymatically isolated from the descending thoracic aorta of euthanized male Sprague Dawley rats using carbon dioxide (CO<sub>2</sub>) asphyxiation and seeded onto 60 mm plastic dishes (Corning, Corning, NY). Cells were maintained in a DMEM-F12 (Invitrogen) medium supplemented with 10% fetal bovine serum (FBS, ATLANTA Biologicals, Lawrenceville, GA) in a humidified incubator with 5% CO<sub>2</sub> at 37 °C.<sup>29</sup>

## 2.2. ECM Protein-Coated Polyacrylamide Gel Substrate Preparation.

PA gel substrates were prepared according to the protocol adapted from Fischer et al.<sup>30</sup> Briefly, 50 mm glass-bottom dishes (MatTek Corporation, Ashland, MA) were activated by drying a small amount of 0.1 N sodium hydroxide at 37 °C, followed by grafting a single layer of (3-aminopropyl) triethoxysilane (Sigma, St Louis, MO). The aminated surface was then coated with 0.5% glutaraldehyde to serve as a crosslinker for the PA gel. PA solutions were prepared using 40% acrylamide (ACR), 2% Bis-ACR solution, 10% tetramethylethylenediamine (TEMED), and 10% ammonium persulfate (APS, Sigma; ACR, Bis-ACR, and TEMED from BIO-RAD) such that the resulting gels were 3.5 kPa (5% acrylamide (ACR), 1% Bis/ACR), 28 kPa (15% ACR, 2.5% Bis/ACR), and 103 kPa (15% ACR, 3.5% Bis/ACR). PA gel polymerization was catalyzed with 0.05% APS and 0.1% TEMED. Coverslips were deactivated using a small volume of dimethyldichlor-*o*-silane (Sigma, St. Louis, MO). The PA solution was pipetted onto the activated glass-bottom dishes, covered with a deactivated coverslip, and allowed to polymerize under vacuum for 30 min. The resulting PA gels were then washed several times with 50 mM 4-(2-hydroxyethyl)-1-piperazineethanesulfonic acid buffer (HEPES, ThermoFisher Scientific, Waltham, MA) to remove the unreacted monomer. The PA gel surface was coated with 1 mM sulfosuccinimidyl 6-(4'-azido-2'-nitrophenylamion) hexanoate (ThermoFisher Scientific, Waltham, MA) in HEPES and activated under 20 min of UV light and served as the crosslinker between the PA gel and ECM proteins. After quick washes with HEPES, the gel surface was then grafted with one layer of either COL1 (Sigma, St. Louis, MO) (0.15 mg/mL) or FN (Invitrogen, Carlsbad, CA) (0.15 mg/mL). The ECM protein coatings were evaluated by immunostaining and imaging on a confocal microscope (Figure S1). PA gel stiffness was determined by AFM indentation, as previously described.<sup>28,31</sup>

## 2.3. Cell Migration Studies.

At 70% confluency, P0 cells were trypsinized and seeded onto COL1- or FN-coated gel substrates at a density of 10 000 cells/cm<sup>2</sup>. Cells were allowed to plate in serum-free media for 2 h in a humidified incubator with 5% CO<sub>2</sub> at 37 °C. Cell migration studies were carried out using a JuLI Stage Real-Time Cell History Recorder (NanoEnTek Inc., Seoul, Korea) maintained in a humidified incubator with 5% CO<sub>2</sub> at 37 °C. Regions of interest with a sufficient number of nontouching cells were preselected and imaged with a 4× or 10× objective at 10–15 min intervals over the course of 24 h. Image stacks were processed using FIJI (FIJI is Just ImageJ). The plugin StackReg (Biomedical Imaging Group, Swiss Federal Institute of Technology Lausanne) was used to align image stacks, and cell tracking was done manually using the built-in MtrackJ plugin. Position data was processed using MATLAB, and any tracked cell with a final displacement of less than 10 μm was eliminated from analysis (R2016a, MathWorks Inc., Natick, MA). The random motility coefficient (RMC) was calculated by a linear curve fit of mean square displacement (MSD) vs time using eq 1

$$\text{MSD} = 4\mu t \quad (1)$$

where  $\mu$  is the RMC, and  $t$  is time.<sup>32</sup>

## 2.4. Confocal Imaging and Image Processing.

Primary VSMCs were seeded onto PA gels at a density of 10 000 cells/cm<sup>2</sup>. At 60 to 80% confluency, VSMCs were fixed using 4% paraformaldehyde solution in phosphate-buffered saline (PBS) (Affymetrix, CA) for 20 min at room temperature and rinsed with PBS. Cells were permeabilized with 0.1% Triton X-100 in PBS for 5 min followed by two rinses with PBS. A 1:1000 dilution of phalloidin (Phalloidin-iFluor 488, Abcam, Cambridge, U.K.) in 1% bovine serum albumin/PBS was used to stain the F-actin cytoskeleton for 20 min. Following two more washes with PBS, the nucleus was counterstained using a 1:1000 dilution of Hoechst 33342 (BD Biosciences, San Jose, CA) dissolved in PBS for 10 min. VSMCs were imaged using a laser scanning confocal microscope (Olympus IX83 FV1200, Olympus Life Science) at a 1024 × 1024 pixel resolution and *z*-height of 0.38 μm. *Z*-stacks were flattened and manually segmented by tracing VSMCs in contact with at least one other cell. As previously described, a series of elongated Laplacian-of-Gaussian (eLoG) filters were used to convolve flattened *z*-stacks to detect total cellular cytoskeletal fiber orientation.<sup>28,29</sup>

## 2.5. Live VSMC AFM Imaging and Cytoskeletal Orientation Processing.

Contact mode live AFM imaging (MFP-3D-BIO, Asylum Research, Santa Barbara, CA) was used to study live VSMC topography. A 30 × 30 μm area of the cell surface was scanned at a digital density of 512 × 512 pixels using a stylus AFM probe (model MLCT-C, *k* = 15 pN/nm, Bruker, Santa Barbara, CA). The cell surface scanning frequency was 0.3 Hz. All experiments were conducted in the CO<sub>2</sub>-independent medium at room temperature for a period of 1–2 h.<sup>28,31</sup> AFM height images were used to compute actin stress fiber density (Figure S2). AFM deflection images were used to compute VSMC cortical actin stress fiber orientation using a modified method of Karlon et al. (Figure S3).<sup>33</sup>

## 2.6. Statistical Analysis.

Statistically significant differences between substrates of differing stiffness were determined using a one-way analysis of variance (ANOVA) on Origin Pro 8.1 (OriginLab Corporation, Northampton, MA). Significant differences in stress fiber orientation were assessed using Student's *t*-test on the circular variance of each experimental group of VSMCs. A value of \**P* 0.05, \*\**P* 0.01, and \*\*\**P* 0.001 was considered statistically significant. All data were reported as mean ± standard error of the mean (SEM).

# 3. RESULTS

## 3.1. Effect of Substrate Stiffness and Extracellular Matrix Proteins on Vascular Smooth Muscle Cell Migration Distance.

An overview schematic showing the methodology for the migration experiments can be seen in Figure 1A. Using the manually tracked positions of the nuclei, cell tracks for each gel were mapped to a common origin (Figure 1B). Qualitatively, VSMCs on the FN-coated 103 kPa gel had the greatest migration distance overall, with the FN-coated gels appearing to show an increase in migration as stiffness increased. Furthermore, the Gaussian curve fit of

the migration histograms showed the peak shifting to the left as stiffness increased on COL1-coated gels, indicating that cells traversed a shortened distance (Figure 2A–C).

The opposite effect was observed on the FN-coated gels with the peak shifting to the right as stiffness increased, indicative of a greater migration distance (Figure 2D–F). The 103 kPa COL1 and 3.5 kPa FN, which were the substrates that exhibited the lowest migration distance, also had the narrowest peak, whereas peaks were broader for the substrates with higher migration distances. The average distance vs time plots also showed this trend with the migration distance increasing as substrate stiffness decreased for COL1 and the inverse trend for FN (Figure 3A,B). Statistical testing with one-way ANOVA showed that substrate stiffness had a significant effect on migration distance on both COL1- and FN-coated substrates ( $P < 0.05$ ) (Figure 3C,D).

### 3.2. Effect of Substrate Stiffness and Extracellular Matrix Proteins on Vascular Smooth Muscle Cell Migration Dynamics.

VSMC migration dynamics were characterized by analyzing migration speed and stoppages. From the distance vs time graphs for individual cells, a stepwise migratory behavior was noted, where there would be rapid increases in distance traveled followed by a much slower increase of complete stops (representative plot in Figure 4A). The derivative of this plot confirmed this behavior with the number of local speed peaks observed at regular intervals, demonstrating an oscillatory migration behavior (Figure 4B). Average migration speed for COL1 (Figure 4C) was found to significantly decrease with increasing stiffness while FN-coated substrates (Figure 4F) showed the opposite trend with average speed increasing with increasing stiffness, matching the migration distance results. The migration stops were also analyzed for each cell. The number of stops was counted, and consecutive stops were merged together. COL1-coated substrates had the greatest number of stops on 103 kPa substrates, and stiffness was found to have a significant effect on the number of stops, with an increasing trend seen with increasing stiffness (Figure 4D). The opposite trend was seen with FN-coated substrates. The 3.5 kPa substrate had the highest number of stops, and a significant downward trend in the number of stops was seen with increasing stiffness (Figure 4G). For the resting time (total time stopped), the lengths of all stops were added together. Substrate stiffness was also shown to have a significant effect on the resting time for both proteins, following the same trend as migration distance with total resting time increasing on COL1-coated substrates (Figure 4E) and decreasing on FN-coated substrates with increasing substrate stiffness (Figure 4H).

From the displacement data, the MSD was calculated for each time point and averaged across all cells. On COL1-coated gels, the average MSD for both 3.5 and 28 kPa substrate tracked almost identically, while for the 103 kPa substrate, the MSD was consistently higher although error bars still overlapped (Figure 5A). This result stands in contrast to migration distance for COL1 as the 103 kPa substrate had the lowest average distance. For FN, the 28 kPa substrate initially had a higher MSD than the 3.5 kPa substrate but the difference ended after about 800 min (Figure 5B). VSMCs cultured on the 103 kPa FN-coated substrates maintained the highest MSD among all three substrates. From the MSD, the RMC was

calculated, and substrate stiffness had a significant effect on the RMC for FN-coated substrates (Figure 5D) but not for COL1-coated substrates (Figure 5C).

### 3.3. ECM Composition did Not Alter Global VSMC Cytoskeletal Architecture in Response to Changes in Substrate Stiffness.

To test whether overall cytoskeletal architecture was altered in response to ECM composition and substrate stiffness, fluorescent images of the actin cytoskeleton were obtained by confocal microscopy. Representative *z*-stack images of actin stress fibers are shown in Figure 6 (top rows, panels A and B) for COL1- and FN-coated gel substrates with an E-modulus of 3.5 kPa (left), 28 kPa (middle), and 103 kPa (right). The corresponding stress fiber orientation color maps (Figure 6A,B, bottom rows) were computed using a proprietary MATLAB software. VSMCs on the 28 and 103 kPa substrates showed a fairly consistent mix of colors for each cell for a given ECM coating, indicating substrate stiffness had little or no effect on global cytoskeletal arrangement. However, a potential effect was observed with VSMCs on the COL1-coated 3.5 kPa substrate, with the cells displaying more varied colors. F-actin orientation was quantitatively analyzed and plotted in histograms. The results confirmed our qualitative assessment of the color maps that substrate stiffness had an effect on cytoskeletal architecture on COL1-coated substrates but not the FN-coated substrates (Figure 6C,D, respectively). In addition, VSMCs on the FN-coated substrates did show a more dispersed F-actin orientation than those on the COL1-coated substrates. The quantified group data showed a significant difference in global actin stress fiber alignment along the dominant orientation angle ( $-10$ – $10^\circ$ ) between the COL1-coated substrates, with VSMCs on the 3.5 kPa showing a more dispersed orientation while no significant difference was observed on the FN-coated substrates (Figure 6E,F, respectively).

### 3.4. Live AFM Imaging-Revealed ECM Composition Induces Differential Effects of Substrate Stiffness on VSMC Cytoskeletal Orientation.

To examine if the observed changes in VSMC migration on COL1- and FN-coated PA gels were correlated with differences in the cortical cytoskeletal architecture, live cell AFM imaging was used. As opposed to confocal microscopy, which shows the whole actin cytoskeleton, AFM contact mode scans only the outermost cortical stress fibers.<sup>28,29,31</sup> Representative AFM height images of stress fibers are shown in Figure 7 for VSMCs cultured on COL1- (top rows of panel A) and FN (top rows of panel B)-coated substrates. The bottom row of each panel shows the stress fiber area fraction of each image, with the red representing the area occupied by stress fibers and the blue representing the background. No significant difference in the stress fiber area fraction between the different substrate stiffnesses for both COL1-coated (Figure 7C) and FN-coated gel substrates was found, indicating that the amount of stress fibers did not vary (Figure 7D). In addition, no significant difference in average roughness was seen between the 28 and 103 kPa substrates for both COL1 and FN (Figure 7E,F, respectively).

Representative AFM deflection images are presented in Figure 8 for the cells cultured on the COL1- (panel A, top row) and FN-coated (panel B, top row) substrates, respectively. The corresponding circular histogram for each deflection image was displayed in the bottom row. Stress fiber orientation angles were normalized along the most dominant orientation angle

frequency to allow for comparison across groups. The COL1-coated 28 kPa substrate shows a much broader variety of fiber orientation angles (panel A, bottom left) compared to the tight grouping seen on the 103 kPa substrate (panel A, bottom right), indicating an increase in stress fiber orientation for the stiffer substrate. Qualitatively, for FN-coated substrates, the 103 kPa substrate (Figure 8B, bottom left) shows a more dispersed angle grouping compared to the 28 kPa substrate (Figure 8B, bottom right), indicating a more disorganized stress fiber architecture. The summarized stress fiber orientation corroborated the qualitative analysis of the deflection images, showing a clear increase in stress fiber alignment with increased stiffness for the COL1-coated substrate (Figure 8C) and a clear decrease for the FN-coated substrate (Figure 8D). From the summarized percent frequency of the stress fibers with the dominant orientation angle ( $-20$ – $20^\circ$ ), increasing substrate stiffness was found to significantly increase stress fiber alignment for the COL1-coated substrate (Figure 8E) and conversely result in a significant stress fiber dispersion for the FN-coated substrate (Figure 8F).

#### 4. DISCUSSION

Cell migration is a well-studied phenomenon, and the importance of ECM stiffness and composition has been known for a long time.<sup>34,35</sup> However, reported effects were highly variable, even contradictory, depending on the cell type used. Bangasser et al. reported that U251 glioma cells exhibited a peak RMC on a 100 kPa COL1-coated substrate.<sup>32</sup> Others have reported lower migration of MDA-MB-231 cells on irradiated collagen substrates with reduced stiffness.<sup>36</sup> Meanwhile, human keratinocytes have been found to have a higher migration velocity on a 1.2 kPa digested COL1-coated substrate than on a 24 kPa substrate.<sup>37</sup> Differences were also observed for FN-coated substrates where no changes in migration were found for mouse enteric neural crest cells on substrates with stiffness ranging from 1.5 kPa to GPa,<sup>38</sup> while both fibroblasts and neutrophils exhibited lower migration distances with increasing stiffness.<sup>34,39</sup> Others have shown an increased migration speed of human adipose-derived stem cells with increasing substrate stiffness.<sup>40</sup> Interestingly, in the aforementioned study with neutrophils, Oakes et al. reported that although migration velocity decreased with increasing stiffness, neutrophils on stiff substrates had a higher MSD, indicating they migrated with greater persistence.<sup>39</sup> In this study, we provide further insight into the effects of substrate stiffness and composition on cell migration specifically with VSMCs by mimicking atherosclerotic microenvironments.

We found that the migration distance and speed on COL1-coated substrates decreased with increasing substrate stiffness, with other dynamical properties behaving as would be expected for the observed decrease in migration (Figures 3 and 4). Interestingly, although not significant, the 103 kPa COL1-coated substrate did exhibit the highest MSD and RMC, indicating that despite migrating slower, VSMCs on the stiff substrate did migrate with greater persistence, as was reported on FN-coated substrates (Figure 5).<sup>39</sup> In addition, an oscillatory-like behavior was seen in the migration speed (Figure 4), potentially relating to oscillations in cell stiffness we have previously found. Spontaneous oscillations in cell elasticity have been linked to myosin II activity, which plays a critical role in the contraction of the cell during migration.<sup>22,41</sup> The decrease in migration distance on the stiffer COL1-coated substrates correlates well with the behavior of VSMCs during atherogenesis, where



VSMCs migrate from the less stiff media to the stiffer fibrous cap. During the formation of the fibrous cap in the middle stages of atherogenesis, VSMCs secrete abundant amounts of fibrous COL1, which stabilizes the fibrous cap and has been shown to downregulate migration-related genes.<sup>42–46</sup> Our results demonstrate that the simultaneous stiffening of the cap during these stages may contribute to a decrease in VSMC migration and help to stabilize the plaque. As the plaque progresses to a late-stage atheroma, macrophages accumulate in the shoulder regions of the plaque, secreting matrix metalloproteinases (MMPs).<sup>43,45</sup> MMPs degrade the COL1-rich ECM and along with the loss of VSMCs, causing the fibrous cap to thin and become prone to rupture in late-stage atherosclerosis.<sup>42,46</sup> Monomeric and fragmented COL1 resulting from the degradation of the fibrous cap have been shown to stimulate VSMC migration.<sup>43</sup> Apoptosis has been identified as a primary cause of VSMC loss within the fibrous cap due to the activity of activated inflammatory cells.<sup>47</sup> However, based on our results, the degradation of COL1 would lower the stiffness of ECM and could further stimulate VSMC migration toward regions of greater stiffness and thus also contribute to fibrous cap thinning and subsequent plaque rupture. Migration on FN-coated substrates was found to be similar to some previously reported results, with migration distance and speed increasing with increasing stiffness (Figures 3 and 4).<sup>40</sup> Large amounts of FN have been previously noted in the fatty streaks of early atherosclerosis.<sup>48,49</sup> The increased FN has been shown to be vital not only for further atherosclerotic progress but also in the formation of the fibrous cap, despite being nearly absent within the fibrous cap.<sup>50</sup> FN-rich COL1-poor deposits have been found in some plaques with subendothelial cells being concentrated to these areas.<sup>48</sup> The ECM of atherosclerotic arteries has also been found to contain abundant deposits of FN with extra domain A that has been shown to promote atherosclerosis.<sup>51</sup> Based on our results, these FN deposits along with the increased stiffness of atherosclerotic arteries may contribute to the VSMC migration seen in the progression of atherosclerosis. In addition, both MSD and RMC increased with increasing stiffness, indicating that VSMCs not only migrated a greater distance but also had greater persistence (Figure 5). Meanwhile, the number of stops and resting time decreased with increasing stiffness as anticipated for the increase in migration distance on stiffer substrates (Figure 4G,H). It should be noted that although the PA gels were coated with equal concentrations of COL1 and FN, cells have been shown to exhibit different migratory responses to the same level of different proteins.<sup>52–55</sup> In particular, human smooth muscle cells displayed peak migration on FN at a coating concentration around 20  $\mu\text{g}/\text{mL}$  and lower migration at higher concentrations<sup>52</sup> while 3T3 fibroblast migration peaked at a COL1 coating concentration of 0.15  $\text{mg}/\text{mL}$ .<sup>53</sup> Furthermore, substrate stiffness and ECM protein density have been shown to modulate mechanotransduction, with behavior varying by ECM protein.<sup>56</sup> Thus, the observed differences could be due in part to the amount of protein present and further studies varying the protein-coating concentration are required to examine this question.

Our results indicate how VSMCs respond to environments of different stiffness may depend on the ECM protein present. Numerous studies have shown that migration behavior may depend on ECM proteins.<sup>17–19</sup> Recently, we have also shown that VSMCs cultured on COL1 and FN have different responses to fluvastatin, which was linked to integrin adhesion and expression.<sup>57</sup> It is widely known that cells bind to different ECM proteins through different integrins.<sup>58</sup> These integrin–ECM protein binding pairs are known to vary in

binding strength and dynamics.<sup>55,59</sup> Talin has been shown to be critical to integrin adhesion function by binding directly to actin, inducing integrin activation, and is mechanosensing, unfolding in response to large enough forces enabling the recruitment of other proteins such as vinculin.<sup>60</sup> Some evidence suggests that some integrin may be mechanosensitive.<sup>61</sup> Thus, it is possible that the different integrins' binding to different ECM proteins could have varied mechanosensitivity and thus exhibit different responses to substrate stiffness. It is also not clear what effect COL1 and FN together would have on VSMC migration as other studies have shown that one ECM protein can completely mask the effect of another.<sup>18,19</sup>

Cytoskeletal remodeling in response to changes in substrate stiffness and membrane cholesterol manipulation has been reported.<sup>28</sup> Thus, we thought that cytoskeletal remodeling could also be linked to ECM composition, which may influence VSMC migration. Global stress fiber orientation was first analyzed by confocal microscopy. Substrate stiffness was shown to have no effect on actin stress fiber alignment for the FN coatings while a significant effect was observed on the COL1-coated substrates. In addition, VSMCs on FN-coated substrates did have a notably more dispersed actin alignment compared to those on COL1 (Figure 6). To more closely analyze only the cortical actin stress fibers, AFM contact mode imaging was employed. Since the AFM tip is only able to indent several nanometers into the cell surface, it is able to detect only the stress fibers closest to the surface. These fibers hold the most relevance for cell migration as they are linked to focal adhesion through the proteins vinculin and talin.<sup>21,22</sup> Our results demonstrate that substrate stiffness had a significant effect on cortical VSMC stress fiber orientation for both COL1- and FN-coated substrates (Figure 8). However, VSMCs cultured on COL1 had an increase in stress fiber orientation on the stiffer substrate, while those cultured on FN displayed a decrease in the organization, similar to previously reported results.<sup>28,34</sup> Furthermore, for both COL1 and FN, VSMCs with the more disorganized stress fiber orientation exhibited a higher migration distance. It is plausible that increased F-actin polymerization at the leading edge of faster VSMCs leads to a decrease in stress fiber orientation.<sup>28</sup> The observed difference in global and cortical stress fiber architecture could be due to the linkage of cortical F-actin to mechanosensing integrins via talin in FAs, which have been shown to co-align with F-actin and grow parallel to strain.<sup>62</sup>

## 5. CONCLUSIONS

In summary, we found that VSMC migration was dependent on both substrate stiffness and ECM protein composition. Higher migration distance was also linked to a more disorganized actin cytoskeleton architecture. These results support our hypothesis that ECM stiffness and composition coordinate to regulate cell migration dynamics and cytoskeleton architecture. Our results also provide further insight into the effects of the heterogeneous microenvironments seen in aging and atherosclerotic plaques on disease progression. In future studies, we aim to also study the effect of cholesterol on VSMC migration in conjunction with ECM stiffness and composition potentially using ApoE mice or manipulating cholesterol using statins and oxidized low-density lipoprotein while also employing a three-dimensional model to better mimic atherosclerotic microenvironments.

## Supplementary Material

Refer to Web version on PubMed Central for supplementary material.

## ACKNOWLEDGMENTS

This work was supported in part by the American Heart Association (15SDG25420001 (Z.H.)), the South Dakota Board of Regents (UP1600205 (Z.H.)), the National Science Foundation/EPSCoR Cooperative Agreement (IIA-1355423), and NIH (R15HL147214 (Z.H.)).

## REFERENCES

- Bennett MR; Sinha S; Owens GK Vascular Smooth Muscle Cells in Atherosclerosis. *Circ. Res* 2016, 118, 692–702. [PubMed: 26892967]
- Monk BA; George SJ The Effect of Ageing on Vascular Smooth Muscle Cell Behaviour—A Mini-Review. *Gerontology* 2015, 61, 416–426. [PubMed: 25471382]
- Schwartz SM; Virmani R; Rosenfeld ME The good smooth muscle cells in atherosclerosis. *Curr. Atheroscler. Rep* 2000, 422–429. [PubMed: 11122774]
- Tesauro M; Mauriello A; Rovella V; Annicchiarico-Petruzzelli M; Cardillo C; Melino G; Di Daniele N Arterial ageing: from endothelial dysfunction to vascular calcification. *J. Intern. Med* 2017, 281, 471–482. [PubMed: 28345303]
- Allahverdian S; Chehroudi AC; McManus BM; Abraham T; Francis GA Contribution of intimal smooth muscle cells to cholesterol accumulation and macrophage-like cells in human atherosclerosis. *Circulation* 2014, 129, 1551–1559. [PubMed: 24481950]
- Tracqui P; Broisat A; Toczek J; Mesnier N; Ohayon J; Riou L Mapping elasticity moduli of atherosclerotic plaque in situ via atomic force microscopy. *J. Struct. Biol* 2011, 174, 115–123. [PubMed: 21296163]
- Akyildiz AC; Speelman L; Gijzen FJ Mechanical properties of human atherosclerotic intima tissue. *J. Biomech* 2014, 47, 773–783. [PubMed: 24529360]
- Tesauro M; Mauriello A; Rovella V; Annicchiarico-Petruzzelli M; Cardillo C; Melino G; Di Daniele N Arterial ageing: from endothelial dysfunction to vascular calcification. *J. Intern. Med* 2017, 281, 471–482. [PubMed: 28345303]
- Bordeleau F; Mason BN; Lollis EM; Mazzola M; Zanotelli MR; Somasegar S; Califano JP; Montague C; LaValley DJ; Huynh J; Mencia-Trinchant N; Negron Abril YL; Hassane DC; Bonassar LJ; Butcher JT; Weiss RS; Reinhart-King CA Matrix stiffening promotes a tumor vasculature phenotype. *Proc. Natl. Acad. Sci. U.S.A* 2017, 114, 492–497. [PubMed: 28034921]
- Lee PF; Bai Y; Smith RL; Bayless KJ; Yeh AT Angiogenic responses are enhanced in mechanically and microscopically characterized, microbial transglutaminase crosslinked collagen matrices with increased stiffness. *Acta Biomater.* 2013, 9, 7178–7190. [PubMed: 23571003]
- Lakatta EG Arterial and cardiac aging: major shareholders in cardiovascular disease enterprises: Part III: cellular and molecular clues to heart and arterial aging. *Circulation* 2003, 107, 490–497. [PubMed: 12551876]
- Wang M; Zhao D; Spinetti G; Zhang J; Jiang LQ; Pintus G; Monticone R; Lakatta EG Matrix metalloproteinase 2 activation of transforming growth factor-beta1 (TGF-beta1) and TGF-beta1-type II receptor signaling within the aged arterial wall. *Arterioscler., Thromb., Vasc. Biol* 2006, 26, 1503–1509. [PubMed: 16690877]
- Raines EW The extracellular matrix can regulate vascular cell migration, proliferation, and survival: relationships to vascular disease. *Int. J. Exp. Pathol* 2000, 81, 173–182. [PubMed: 10971738]
- Rocnik EF; Chan BM; Pickering JG Evidence for a role of collagen synthesis in arterial smooth muscle cell migration. *J. Clin. Invest* 1998, 101, 1889–1898. [PubMed: 9576753]
- Scott LE; Mair DB; Narang JD; Feleke K; Lemmon CA Fibronectin fibrillogenesis facilitates mechano-dependent cell spreading, force generation, and nuclear size in human embryonic fibroblasts. *Integr. Biol* 2015, 7, 1454–1465.

16. van Helvert S; Friedl P Strain Stiffening of Fibrillar Collagen during Individual and Collective Cell Migration Identified by AFM Nanoindentation. *ACS Appl. Mater. Interfaces* 2016, 8, 21946–21955. [PubMed: 27128771]
17. Chen WW; Tjin MS; Chua AWC; Lee ST; Tay CY; Fong E Probing the Role of Integrins in Keratinocyte Migration Using Bioengineered Extracellular Matrix Mimics. *ACS Appl. Mater. Interfaces* 2017, 9, 36483–36492. [PubMed: 28967740]
18. Hartman CD; Isenberg BC; Chua SG; Wong JY Vascular smooth muscle cell durotaxis depends on extracellular matrix composition. *Proc. Natl. Acad. Sci. U.S.A* 2016, 113, 11190–11195. [PubMed: 27647912]
19. Hartman CD; Isenberg BC; Chua SG; Wong JY Extracellular matrix type modulates cell migration on mechanical gradients. *Exp. Cell Res* 2017, 359, 361–366. [PubMed: 28821395]
20. Sazonova OV; Isenberg BC; Herrmann J; Lee KL; Purwada A; Valentine AD; Buczek-Thomas JA; Wong JY; Nugent MA Extracellular matrix presentation modulates vascular smooth muscle cell mechanotransduction. *Matrix Biol.* 2015, 41, 36–43. [PubMed: 25448408]
21. Ohashi K; Fujiwara S; Mizuno K Roles of the cytoskeleton, cell adhesion and rho signalling in mechanosensing and mechanotransduction. *J. Biochem* 2017, 161, 245–254. [PubMed: 28082721]
22. Sun Z; Guo SS; Fassler R Integrin-mediated mechanotransduction. *J. Cell Biol* 2016, 215, 445–456. [PubMed: 27872252]
23. Li N; Sanyour H; Remund T; Kelly P; Hong Z Vascular extracellular matrix and fibroblasts-coculture directed differentiation of human mesenchymal stem cells toward smooth muscle-like cells for vascular tissue engineering. *Mater. Sci. Eng., C* 2018, 93, 61–69.
24. Li N; Xue F; Zhang H; Sanyour HJ; Rickel AP; Uttecht A; Fanta B; Hu J; Hong Z Fabrication and Characterization of Pectin Hydrogel Nanofiber Scaffolds for Differentiation of Mesenchymal Stem Cells into Vascular Cells. *ACS Biomater. Sci. Eng* 2019, 5, 6511–6519. [PubMed: 33417803]
25. Li N; Rickel AP; Sanyour HJ; Hong Z Vessel graft fabricated by the on-site differentiation of human mesenchymal stem cells towards vascular cells on vascular extracellular matrix scaffold under mechanical stimulation in a rotary bioreactor. *J. Mater. Chem. B* 2019, 7, 2703–2713. [PubMed: 32255003]
26. Lu X; Ding Z; Xu F; Lu Q; Kaplan DL Subtle Regulation of Scaffold Stiffness for the Optimized Control of Cell Behavior. *ACS Appl. Bio Mater* 2019, 3108–3119.
27. Handorf AM; Zhou Y; Halanski MA; Li WJ Tissue stiffness dictates development, homeostasis, and disease progression. *Organogenesis* 2015, 11, 1–15. [PubMed: 25915734]
28. Sanyour HJ; Li N; Rickel AP; Childs JD; Kinser CN; Hong Z Membrane cholesterol and substrate stiffness co-ordinate to induce the remodelling of the cytoskeleton and the alteration in the biomechanics of vascular smooth muscle cells. *Cardiovasc. Res* 2019, 115, 1369–1380. [PubMed: 30395154]
29. Hong Z; Sun Z; Li M; Li Z; Bunyak F; Ersoy I; Trzeciakowski JP; Staiculescu MC; Jin M; Martinez-Lemus L; Hill MA; Palaniappan K; Meininger GA Vasoactive agonists exert dynamic and coordinated effects on vascular smooth muscle cell elasticity, cytoskeletal remodelling and adhesion. *J. Physiol* 2014, 592, 1249–1266. [PubMed: 24445320]
30. Fischer RS; Myers KA; Gardel ML; Waterman CM Stiffness-controlled three-dimensional extracellular matrices for high-resolution imaging of cell behavior. *Nat. Protoc* 2012, 7, 2056–2066. [PubMed: 23099487]
31. Sanyour H; Childs J; Meininger GA; Hong Z Spontaneous oscillation in cell adhesion and stiffness measured using atomic force microscopy. *Sci. Rep* 2018, 8, No. 2899. [PubMed: 29440673]
32. Bangasser BL; Shamsan GA; Chan CE; Opoku KN; Tuzel E; Schlichtmann BW; Kasim JA; Fuller BJ; McCullough BR; Rosenfeld SS; Odde DJ Shifting the optimal stiffness for cell migration. *Nat. Commun* 2017, 8, No. 15313. [PubMed: 28530245]
33. Karlon WJ; Hsu PP; Li S; Chien S; McCulloch AD; Omens JH Measurement of orientation and distribution of cellular alignment and cytoskeletal organization. *Ann. Biomed. Eng* 1999, 27, 712–720. [PubMed: 10625144]
34. Ghosh K; Pan Z; Guan E; Ge S; Liu Y; Nakamura T; Ren XD; Rafailovich M; Clark RA Cell adaptation to a physiologically relevant ECM mimic with different viscoelastic properties. *Biomaterials* 2007, 28, 671–679. [PubMed: 17049594]

35. Stringa E; Knauper V; Murphy G; Gavrilovic J Collagen degradation and platelet-derived growth factor stimulate the migration of vascular smooth muscle cells. *J. Cell Sci* 2000, 113, 2055–2064. [PubMed: 10806116]
36. Miller JP; Borde BH; Bordeleau F; Zanutelli MR; LaValley DJ; Parker DJ; Bonassar LJ; Pannullo SC; Reinhart-King CA Clinical doses of radiation reduce collagen matrix stiffness. *APL Bioeng.* 2018, No. 031901. [PubMed: 31069314]
37. Zarkoob H; Bodduluri S; Ponnaluri SV; Selby JC; Sander EA Substrate Stiffness Affects Human Keratinocyte Colony Formation. *Cell. Mol. Bioeng* 2015, 8, 32–50. [PubMed: 26019727]
38. Chevalier NR; Gazquez E; Bidault L; Guilbert T; Vias C; Vian E; Watanabe Y; Muller L; Germain S; Bondurand N; Dufour S; Fleury V How Tissue Mechanical Properties Affect Enteric Neural Crest Cell Migration. *Sci. Rep* 2016, 6, No. 20927. [PubMed: 26887292]
39. Oakes PW; Patel DC; Morin NA; Zitterbart DP; Fabry B; Reichner JS; Tang JX Neutrophil morphology and migration are affected by substrate elasticity. *Blood* 2009, 114, 1387–1395. [PubMed: 19491394]
40. Hadden WJ; Young JL; Holle AW; McFetridge ML; Kim DY; Wijesinghe P; Taylor-Weiner H; Wen JH; Lee AR; Bieback K; Vo BN; Sampson DD; Kennedy BF; Spatz JP; Engler AJ; Choi YS Stem cell migration and mechanotransduction on linear stiffness gradient hydrogels. *Proc. Natl. Acad. Sci. U.S.A* 2017, 114, 5647–5652. [PubMed: 28507138]
41. Schillers H; Wälte M; Urbanova K; Oberleithner H Real-time monitoring of cell elasticity reveals oscillating myosin activity. *Biophys. J* 2010, 99, 3639–3646. [PubMed: 21112288]
42. Bentzon JF; Otsuka F; Virmani R; Falk E Mechanisms of plaque formation and rupture. *Circ. Res* 2014, 114, 1852–1866. [PubMed: 24902970]
43. Chistiakov DA; Sobenin IA; Orekhov AN Vascular extracellular matrix in atherosclerosis. *Cardiol. Rev* 2013, 21, 270–288. [PubMed: 23422022]
44. Ponticos M; Smith BD Extracellular matrix synthesis in vascular disease: hypertension, and atherosclerosis. *J. Biomed. Res* 2014, 28, 25–39. [PubMed: 24474961]
45. Rudijanto A The role of vascular smooth muscle cells on the pathogenesis of atherosclerosis. *Acta Med Indones* 2007, 39, 86–93. [PubMed: 17933075]
46. Sakakura K; Nakano M; Otsuka F; Ladich E; Kolodgie FD; Virmani R Pathophysiology of atherosclerosis plaque progression. *Heart, Lung Circ* 2013, 22, 399–411. [PubMed: 23541627]
47. Leskinen MJ; Kovanen PT; Lindstedt KA Regulation of smooth muscle cell growth, function and death in vitro by activated mast cells—a potential mechanism for the weakening and rupture of atherosclerotic plaques. *Biochem. Pharmacol* 2003, 66, 1493–1498. [PubMed: 14555226]
48. Shekhonin BV; Domogatsky SP; Idelson GL; Koteliansky VE; Rukosuev VS Relative distribution of fibronectin and type I, III, IV, V collagens in normal and atherosclerotic intima of human arteries. *Atherosclerosis* 1987, 67, 9–16. [PubMed: 3314885]
49. Holm Nielsen S; Jonasson L; Kalogeropoulos K; Karsdal MA; Reese-Petersen AL; Auf dem Keller U; Genovese F; Nilsson J; Goncalves I Exploring the role of extracellular matrix proteins to develop biomarkers of plaque vulnerability and outcome. *J. Intern. Med* 2020, No. 13034.
50. Rohwedder I; Montanez E; Beckmann K; Bengtsson E; Dunér P; Nilsson J; Soehnlein O; Fässler R Plasma fibronectin deficiency impedes atherosclerosis progression and fibrous cap formation. *EMBO Mol. Med* 2012, 4, 564–576. [PubMed: 22514136]
51. Doddapattar P; Gandhi C; Prakash P; Dhanesha N; Grumbach IM; Dailey ME; Lentz SR; Chauhan AK Fibronectin Splicing Variants Containing Extra Domain A Promote Atherosclerosis in Mice Through Toll-Like Receptor 4. *Arterioscler., Thromb., Vasc. Biol* 2015, 35, 2391–2400. [PubMed: 26427793]
52. DiMilla PA; Stone JA; Quinn JA; Albelda SM; Lauffenburger DA Maximal migration of human smooth muscle cells on fibronectin and type IV collagen occurs at an intermediate attachment strength. *J. Cell Biol* 1993, 122, 729–737. [PubMed: 8335696]
53. Gaudet C; Marganski WA; Kim S; Brown CT; Gunderia V; Dembo M; Wong JY Influence of type I collagen surface density on fibroblast spreading, motility, and contractility. *Biophys. J* 2003, 85, 3329–3335. [PubMed: 14581234]

54. Hayward IP; Bridle KR; Campbell GR; Underwood PA; Campbell JH Effect of extracellular matrix proteins on vascular smooth muscle cell phenotype. *Cell Biol. Int* 1995, 19, 839–846. [PubMed: 8528193]
55. Palecek SP; Loftus JC; Ginsberg MH; Lauffenburger DA; Horwitz AF Integrin-ligand binding properties govern cell migration speed through cell-substratum adhesiveness. *Nature* 1997, 385, 537–540. [PubMed: 9020360]
56. Stanton AE; Tong X; Yang F Extracellular matrix type modulates mechanotransduction of stem cells. *Acta Biomater.* 2019, 96, 310–320. [PubMed: 31255664]
57. Sanyour HJ; Li N; Rickel AP; Torres HM; Anderson RH; Miles MR; Childs JD; Francis KR; Tao J; Hong Z Statin mediated cholesterol depletion exerts coordinated effects on the alterations in rat vascular smooth muscle cell biomechanics and migration. *J Physiol* 2020, No. 9528.
58. Takada Y; Ye X; Simon S The integrins. *Genome Biol.* 2007, 8, 215. [PubMed: 17543136]
59. Chen L; Vicente-Manzanares M; Potvin-Trottier L; Wiseman PW; Horwitz AR The integrin-ligand interaction regulates adhesion and migration through a molecular clutch. *PLoS One* 2012, 7, No. e40202. [PubMed: 22792239]
60. Klapholz B; Brown NH Talin—the master of integrin adhesions. *J. Cell Sci* 2017, 130, 2435–2446. [PubMed: 28701514]
61. Schwartz MA Integrins and extracellular matrix in mechanotransduction. *Cold Spring Harbor Perspect. Biol* 2010, No. a005066.
62. Swaminathan V; Kalappurakkal JM; Mehta SB; Nordenfelt P; Moore TI; Koga N; Baker DA; Oldenbourg R; Tani T; Mayor S; Springer TA; Waterman CM Actin retrograde flow actively aligns and orients ligand-engaged integrins in focal adhesions. *Proc. Natl. Acad. Sci. U.S.A* 2017, 114, 10648–10653. [PubMed: 29073038]

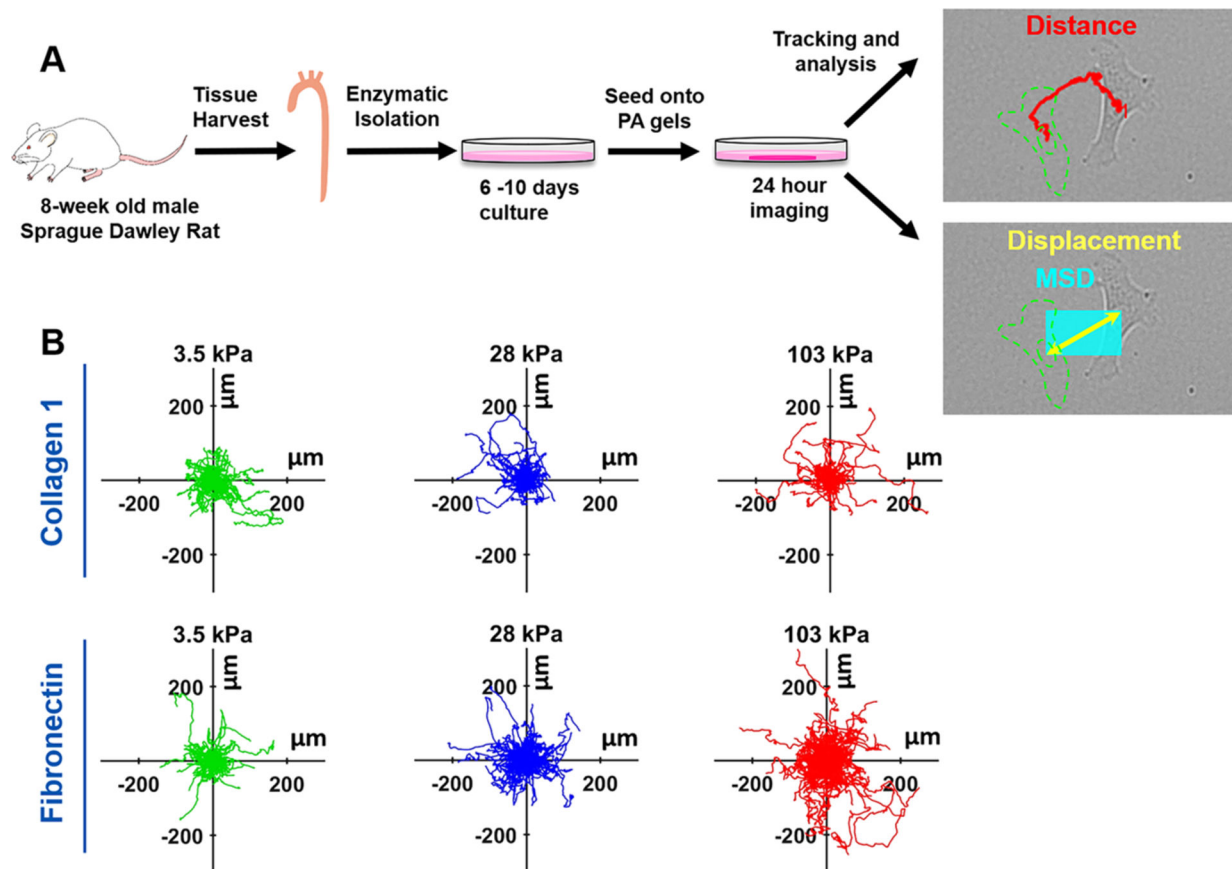


**Figure 1.** VSMC migration on the different ECM protein-coated gel substrates with varying stiffness. (A) Schematic of VSMC migration experiments. The descending thoracic aorta was harvested from 8-week old male Sprague Dawley rats and VSMCs were enzymatically isolated. After 6–10 days of culture, VSMCs were trypsinized and seeded on ECM protein-coated PA gels for 24 h imaging and VSMC positions were tracked. Distance (in red) covers the path the cell took. The displacement (yellow) is the straight-line path from the start point to the end point. Mean square displacement (MSD, cyan) is the square of the displacement, essentially a box covering the area traversed by the cell. (B) Position plot of the VSMC nucleus mapped to a common origin. Top Row: VSMCs on COL1-coated substrates displayed little visual change in migration. Bottom Row: VSMCs on FN-coated substrates show an apparent increase in migration with increasing substrate stiffness. For each stiffness and protein combination, 30 to 50 cells were tracked per independent trial, with three independent replicates.

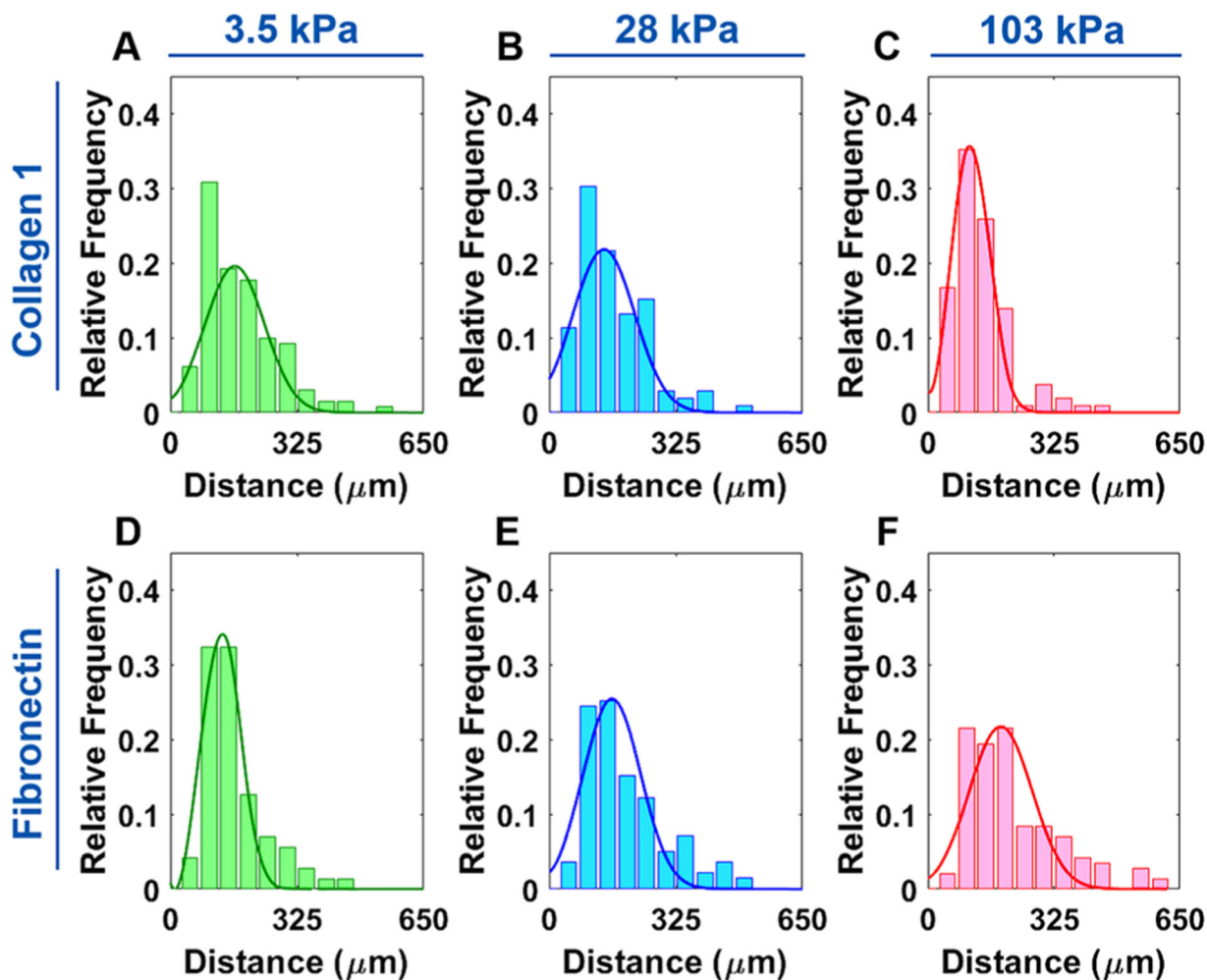


**Figure 2.** Distribution of the VSMC migration distance on different ECM protein-coated gel substrates with varying stiffness. (A–C) VSMCs on the COL1-coated gel substrates. The 103 kPa substrate histogram had a left-shifted, narrower peak than those on the 3.5 and 28 kPa substrates, indicating lower migration distance. (D–F) VSMCs on the FN-coated gel substrates. VSMC migration distances became more dispersed on the stiffer substrates, with the peak shifting to the right, indicating a higher average migration distance.



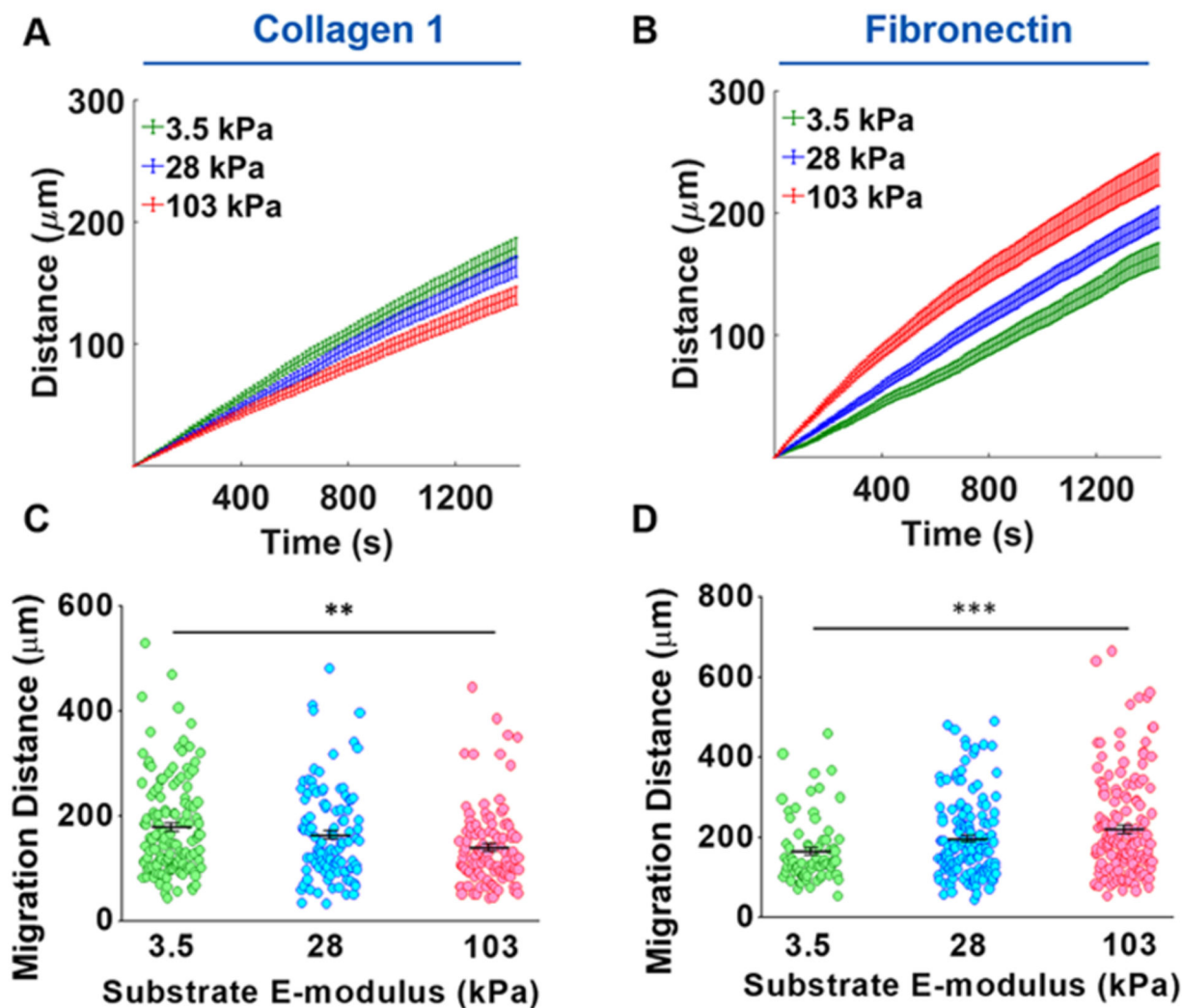


**Figure 3.** Substrate stiffness and ECM composition alter VSMC migration. (A, B) Migration distance vs time plots demonstrated that VSMC migration distance decreased on COL1-coated gels as stiffness increased, while migration distance increased on FN-coated gels with increasing stiffness. (C) Increasing substrate stiffness resulted in a significant decrease in migration distance for COL1-coated substrates. (D) FN-coated substrates showed a significant increase in migration distance with increasing substrate stiffness. Data in panels (A) and (B) are presented as mean migration distance (mid-line) at each time point  $\pm$  SEM. Data were presented in panels (C) and (D) as mean migration distance at end point  $\pm$  SEM. \*\* $P < 0.01$  and \*\*\* $P < 0.001$ .

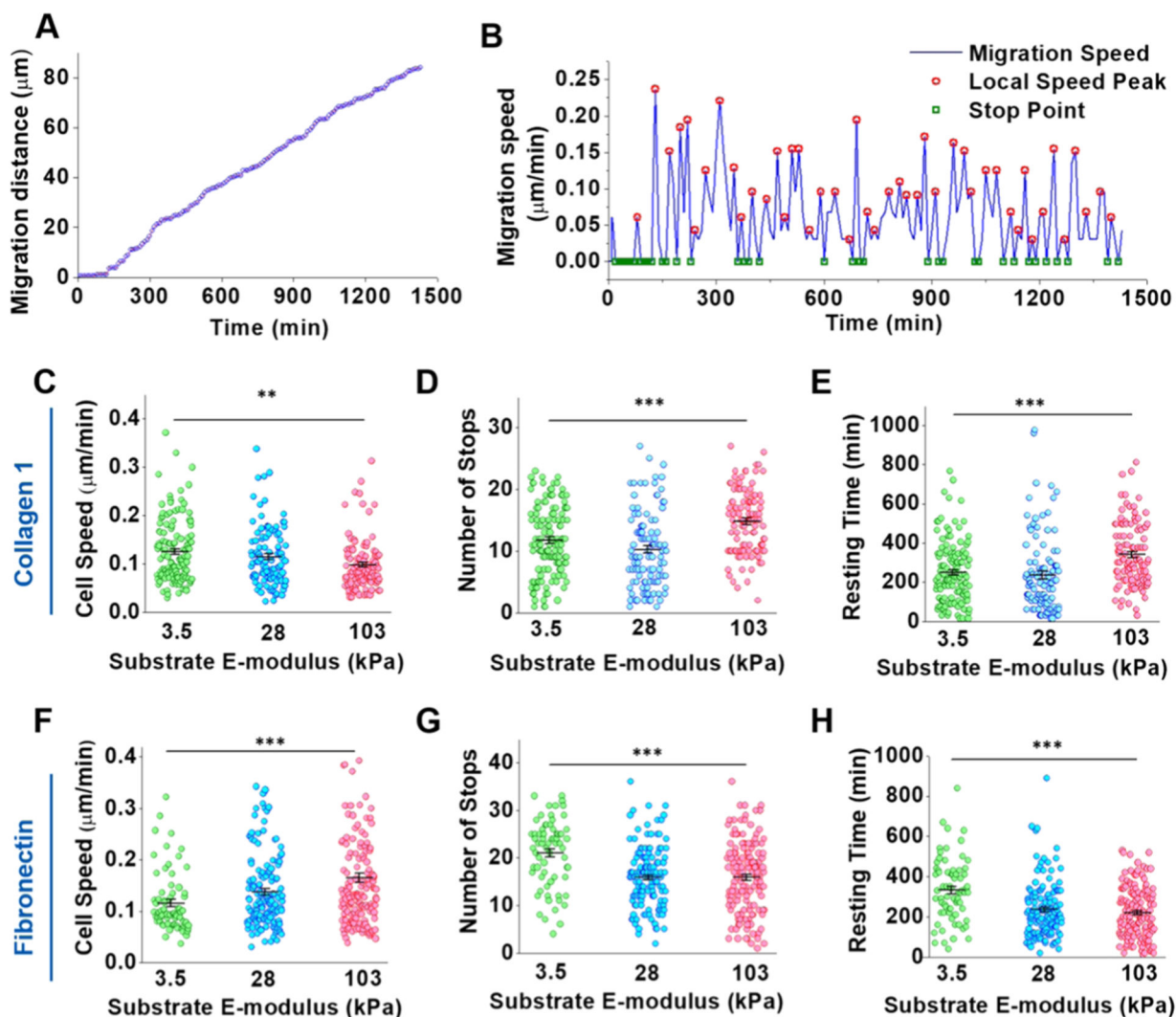


**Figure 4.** Combinatorial effect of ECM proteins and substrate stiffness on VSMC migration dynamics. (A) Representative migration distance vs time plot shows an apparent stepwise migration behavior. (B) Instantaneous migration speeds were determined by the first derivative of the migration distance at each time point. A clear pattern of speed peaks and stops was seen in the migration speed vs time plot. (C, F) VSMC migration speed significantly decreased on COL1 (C) with increasing substrate stiffness. VSMCs on 103 kPa FN-coated (F) substrates displayed significantly higher migration speed than the 28 and 3.5 kPa FN-coated substrates. (D, G) The number of migration stops significantly increased on COL1-coated (D) substrates with increasing substrate stiffness. On FN-coated substrates (G), VSMCs experienced significantly fewer stops on the stiffer gels. (E, H) VSMCs on stiffer COL1-coated substrates (E) stopped for longer resting time. Conversely, the total resting time significantly decreased on the stiffer FN-coated substrates (H). Data were presented as mean  $\pm$  SEM. \*\* $P$  0.01 and \*\*\* $P$  0.001.

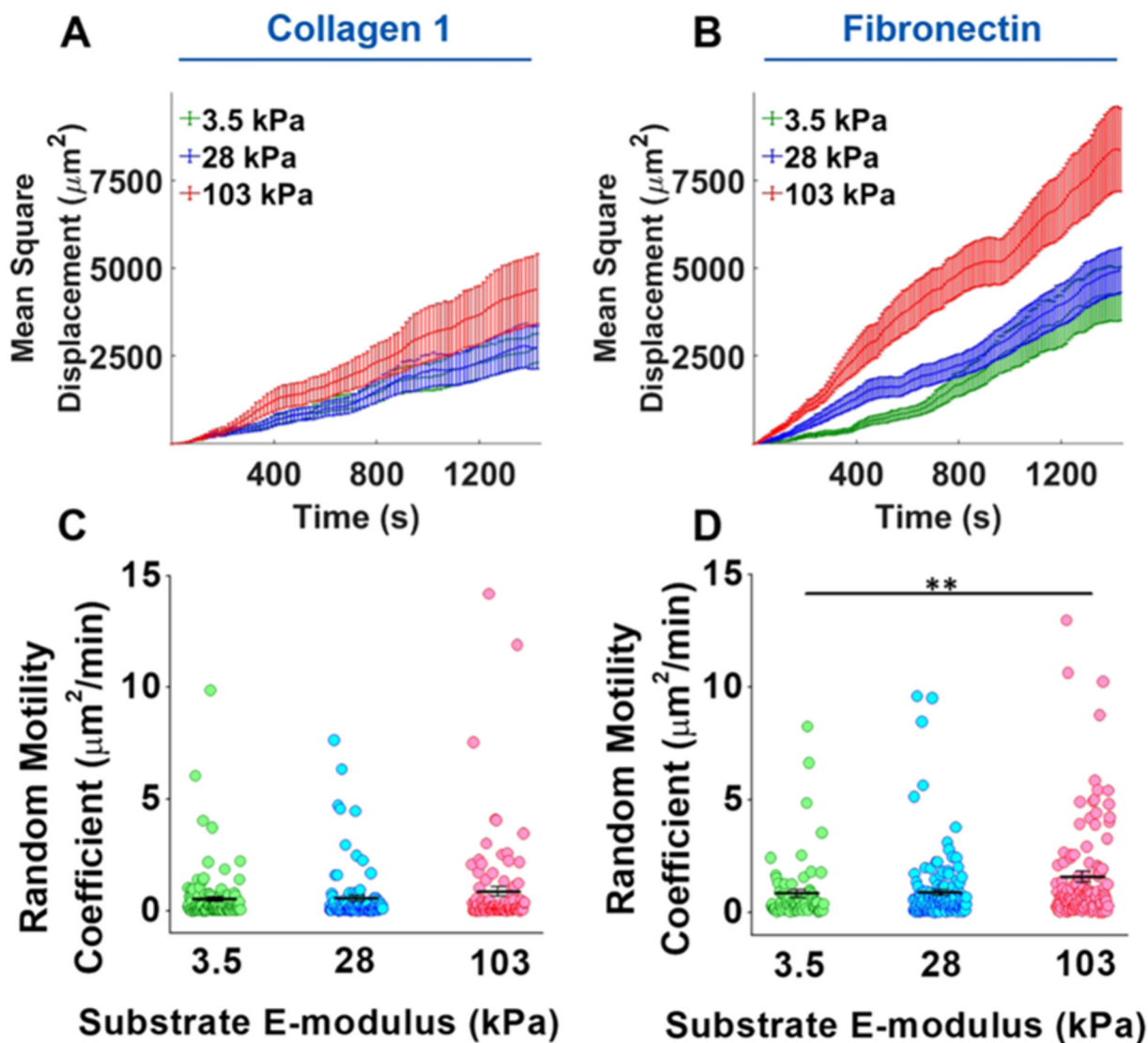


**Figure 5.**

Combinatorial effect of ECM proteins and substrate stiffness on VSMC migration displacement. (A) Despite having the lowest migration distance, VSMCs on the 103 kPa COL1-coated substrate had the highest MSD across all time points, indicating a more persistent migration. (B) VSMCs on the 103 kPa FN-coated substrate also had the highest MSD. (C) Substrate stiffness had no significant effect on the RMC of VSMCs on the COL1-coated substrate. However, VSMCs on the 103 kPa substrate did have the highest RMC. (D) On the FN-coated substrate, substrate stiffness was found to have a significant effect on the RMC. Data were presented as mean  $\pm$  SEM.  $**P < 0.01$ .

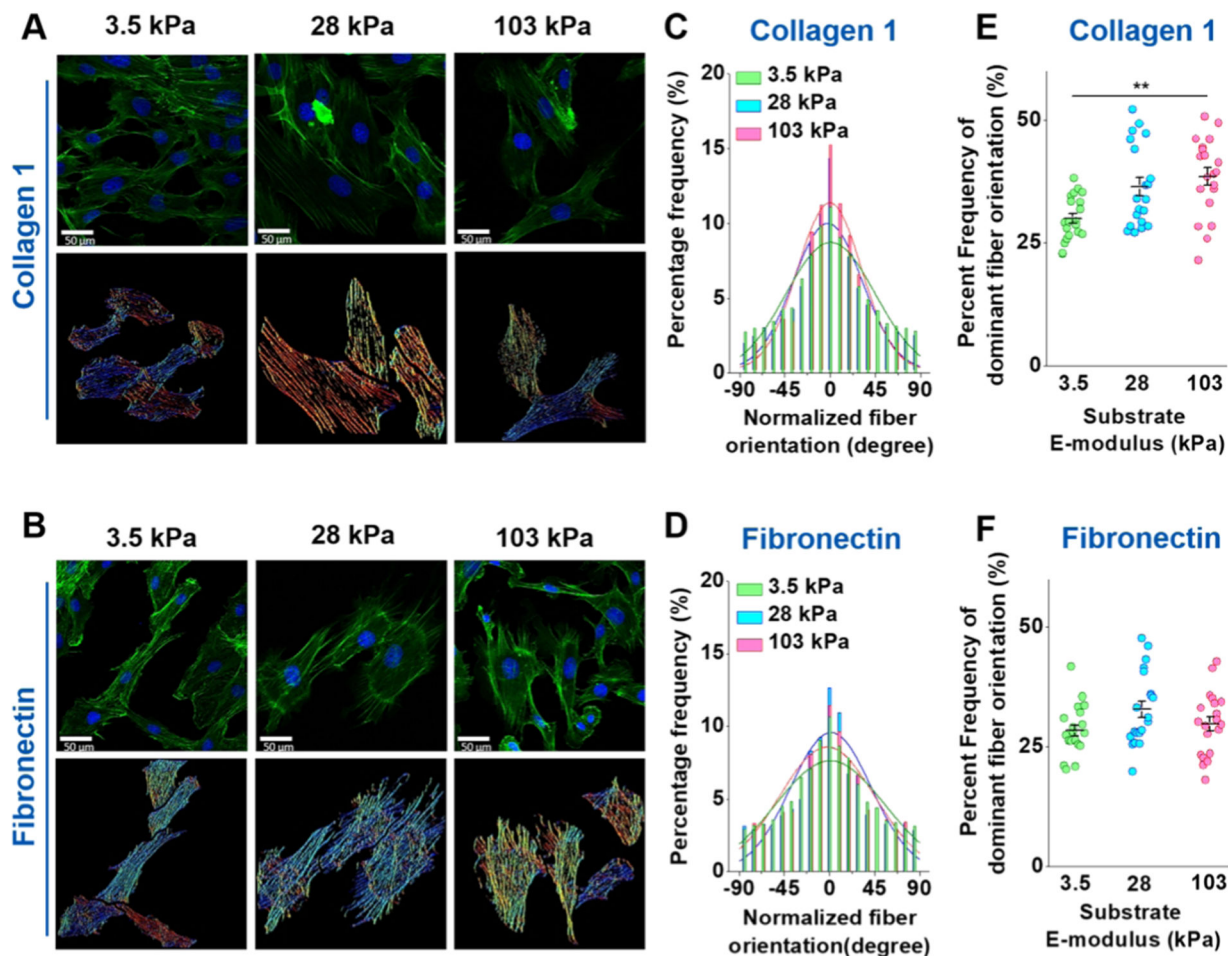


**Figure 6.** Confocal images of the VSMC actin cytoskeleton. (A, B) Top row of each panel shows a representative confocal image of VSMC actin fiber culture on the 3.5 kPa (left), 28 kPa (middle), and 103 kPa (right) substrates for COL1 and FN coatings, respectively. The bottom row of each panel shows the corresponding color map of stress fiber orientation computed from the confocal images. (C, D) Stress fiber orientation histograms for COL1 and FN coating, respectively, where the dominant orientation angle was normalized to zero for each cell. (E, F) Significant difference in the frequency of the dominant orientation angle ( $-10^{\circ}$  to  $+10^{\circ}$ ) was observed for COL1-coated PA gels, with VSMCs on the 3.5 kPa substrate having a more disorganized actin cytoskeleton. No significant difference in the dominant orientation was observed for VSMCs cultured on the FN coatings. Actin (green) was stained with phalloidin and the nuclei (blue) were counterstained with Hoescht. At least 20 confocal images were analyzed for each condition. Data were presented as mean  $\pm$  SEM. **\*\*** $P < 0.01$ .

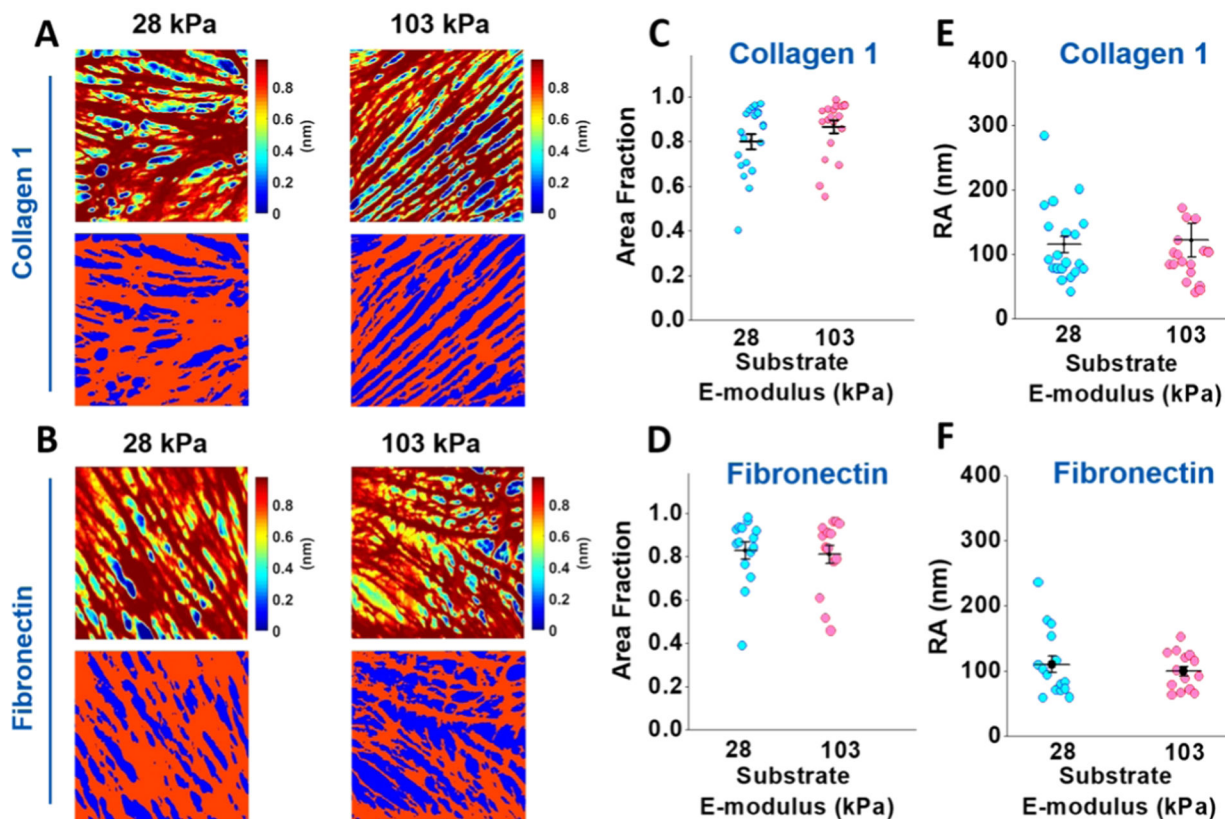


**Figure 7.** AFM height images of the cortical cytoskeleton and the area fraction of the cortical stress fiber. (A, B) Representative AFM height images for VSMCs cultured on COL1- and FN-coated 28 kPa (left) and 103 kPa (right) substrates (top row of panels (A) and (B), respectively). The color changes from blue to red indicate the increasing height of the stress fibers. The bottom row of each panel shows the threshold applied to the height image to separate the areas occupied by stress fibers (red) from the empty background (blue). (C, D) Substrate stiffness did not have a significant effect on the area occupied by stress fibers for the cells cultured on the COL1- or FN-coated substrate. (E, F) Substrate stiffness did not have a significant effect on the average roughness of the cell surface cultured on the COL1- or FN-coated substrate. For AFM imaging, 20 cells cultured on COL1 for each stiffness and 14 cells on FN for each stiffness were imaged. Data were presented as mean  $\pm$  SEM.

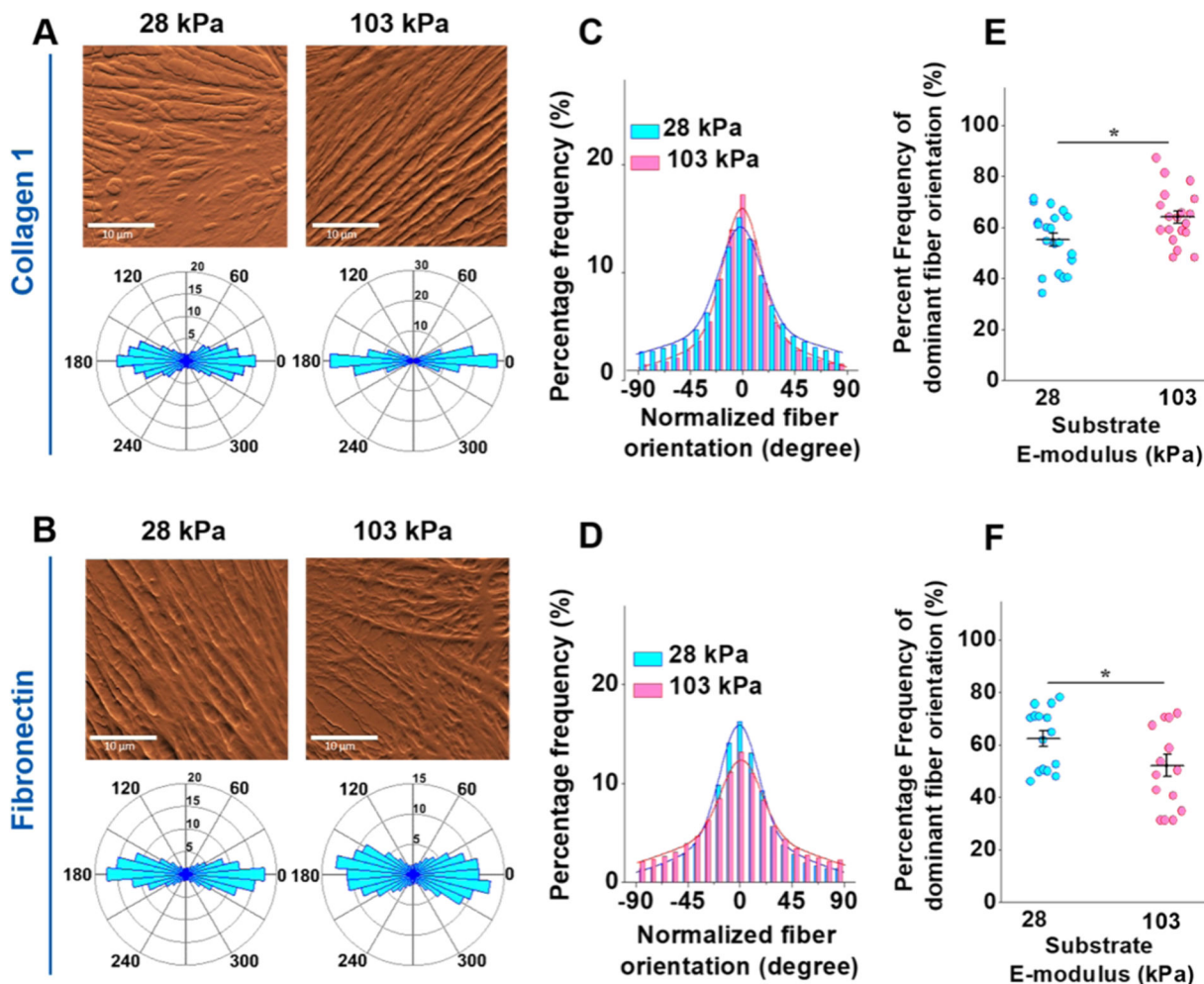


**Figure 8.** Substrate stiffness and ECM coating alter VSMC's cytoskeleton organization. (A, B) Representative  $30 \mu\text{m} \times 30 \mu\text{m}$  AFM deflection images for VSMCs cultured on 28 kPa (left) and 103 kPa (right) are seen in the top row of each panel. The bottom row of each panel displays a circular histogram, showing the normalized stress fiber orientation of each corresponding deflection image. (C) The VSMCs cultured on the 103 kPa COL1-coated substrate displayed a more aligned stress fiber organization than those on the 28 kPa substrate. (D) On FN-coated substrates, VSMCs on the softer 28 kPa substrate displayed the more aligned stress fiber architecture. (E) Summarized percent frequency of dominant fiber orientation ( $-20^\circ \sim +20^\circ$ ) showed a significantly more orientated stress fiber architecture on the 103 kPa COL1-coated substrate. (F) The summarized percentage frequency of dominant fiber orientation ( $-20^\circ \sim +20^\circ$ ) showed the opposite trend for the FN-coated substrate, with VSMCs on the 28 kPa substrate having a more aligned stress fiber orientation. Data were presented as mean  $\pm$  SEM. \* $P < 0.05$ .